PROCEEDINGS OF SCIENCE

Light charged particle production in 96 MeV neutron-induced reactions with oxygen

U. Tippawan[1,2*], S. Pomp[1†], A. Ataç[1], B. Bergenwall[1], J. Blomgren[1], S. Dangtip[1,2], A. Hildebrand[1], C. Johansson[1], J. Klug[1], P. Mermod[1], L. Nilsson[1,4], M. Österlund[1], N. Olsson[1,3], A.V. Prokofiev[4], P. Nadel-Turonski[5], V. Corcalciuc[6], and A.J. Koning[7].

[1]*Department of Neutron Research, Uppsala University, Sweden*
[2]*Fast Neutron Research Facility, Chiang Mai University, Thailand*
[3]*Swedish Defence Research Agency (FOI), Stockholm, Sweden*
[4]*The Svedberg Laboratory, Uppsala University, Sweden*
[5]*Department of Radiation Sciences, Uppsala University, Sweden*
[6]*Institute of Atomic Physics, Heavy Ion Department, Bucharest, Romania*
[7]*Nuclear Research and Consultancy Group NRG, Petten, The Netherlands*
E-mail: udomrat@fnrf.science.cmu.ac.th

In recent years, an increasing number of applications involving fast neutrons have been developed or are under consideration, e.g., radiation treatment of cancer, neutron dosimetry at commercial aircraft altitudes, soft-error effects in computer memories, accelerator-driven transmutation of nuclear waste and energy production.

Data on light-ion production in light nuclei such as carbon, nitrogen and oxygen are particularly important in calculations of dose distributions in human tissue for radiation therapy at neutron beams, and for dosimetry of high energy neutrons produced by high-energy cosmic radiation interacting with nuclei (nitrogen and oxygen) in the atmosphere. When studying neutron dose effects in radiation therapy and at high altitude, it is especially important to consider oxygen, because it is the dominant element (65% by weight) in average human tissue.

In this work, we present experimental double-differential cross sections of inclusive light-ion (p, d, t, ^{3}He and α) production in oxygen, induced by 96 MeV neutrons. Spectra were measured at 8 laboratory angles: 20°, 40°, 60°, 80°, 100°, 120°, 140° and 160°. Measurements were performed at The Svedberg Laboratory (TSL), Uppsala, using the dedicated MEDLEY experimental setup. Deduced energy-differential and production cross sections are reported as well. Experimental cross sections are compared to theoretical reaction model calculations and existing experimental data in the literature.

International Workshop on Fast Neutron Detectors
University of Cape Town, South Africa
April 3 – 6, 2006

* Udomrat Tippawan
† Corresponding author, Tel. +46 18 471 6850, Fax. +46 18 471 3853, E-mail: Stephan.Pomp@tsl.uu.se

PoS(FNDA2006)079

1. Introduction

Recently, there has been increased attention on various applications where fast neutrons play a significant role, like dose effects due to cosmic-ray neutrons for airplane crew [1], fast-neutron cancer therapy [2,3], studies of electronics failures induced by cosmic-ray neutrons [4], accelerator-driven transmutation of nuclear waste and energy production, and determination of the response of neutron detectors. It has been established during recent years that air flight personnel receive among the largest radiation doses in civil work, due to cosmic-ray neutrons. Cancer treatment with fast neutrons is performed routinely at about a several facilities worldwide, and today it represents the largest therapy modality besides the conventional treatments with photons and electrons. Data on light-ion production in light nuclei such as carbon, nitrogen and oxygen are particularly important in calculations of dose distributions in human tissue for radiation therapy at neutron beams, and for dosimetry of high energy neutrons produced by high energy cosmic radiation interacting with nuclei (nitrogen and oxygen) in the atmosphere. These cosmic-ray neutrons also create a reliability problem in modern electronics. A neutron can cause a nuclear reaction inside or near a chip, thus releasing free charge, which in turn could, e.g., flip the memory content or change the result of a logical operation. For all these applications, improved knowledge of the underlying nuclear physics is of major importance.

In this contribution, experimental double-differential cross sections (inclusive yields) for protons, deuterons, tritons, ^{3}He and alpha particles induced by 96 MeV neutrons incident on oxygen [5] are presented. Measurements have been performed at the cyclotron of The Svedberg Laboratory (TSL), Uppsala, using the dedicated MEDLEY experimental setup [6]. Spectra have been measured at 8 laboratory angles, ranging from 20° to 160° in 20° steps. Extrapolation procedures are used to obtain coverage of the full angular distribution and consequently energy differential and production cross sections are deduced. The experimental data are compared to results of calculations with nuclear reaction codes and to existing experimental data in the literature.

2. Experimental Methods

The neutron beam facility at TSL uses the ^{7}Li(p,n)^{7}Be reaction (Q = –1.64 MeV) to produce a quasi-monoenergetic neutron beam [7]. The 98.5 ± 0.3 MeV protons from the cyclotron impinge on the lithium target, producing a full energy peak of neutrons at 95.6 ± 0.5 MeV with a width of 3 MeV FWHM and containing 40% of the neutrons, and an almost constant low-energy tail containing 60% of the neutrons. The neutron beam is directly monitored by a thin-film breakdown counter (TFBC). Relative monitoring can be obtained by charge integration of the proton beam hitting the Faraday cup in the beam dump. The agreement between the two beam monitors was very good during the measurements.

The charged particles are detected by the MEDLEY setup. It consists of eight three-element telescopes mounted inside a 100 cm diameter evacuated reaction chamber. Each telescope has two fully depleted ΔE silicon surface barrier detectors. The thickness of the first ΔE detector (ΔE_1) is either 50 or 60 μm, while the second one (ΔE_2) is either 400 or 500 μm,

and they are all 23.9 mm in diameter (nominal). In each telescope, a cylindrical CsI(Tl) crystal, 50 mm long and 40 mm in diameter, serves as the *E* detector.

A 22 mm diameter 500 μm thick (cylindrical) disk of SiO_2 is used as the oxygen target. For the subtraction of the silicon contribution, measurements using a silicon wafer having a 32·32 mm^2 quadratic shape and a thickness of 303 μm are performed. For absolute cross section normalization, a 25 mm diameter and 1.0 mm thick polyethylene $(CH_2)_n$ target is used. The *np* cross sections at 20° laboratory angle provides the reference cross section [8].

Background events, collected in target-out runs and analyzed in the same way as target-in events, are subtracted from the corresponding target-in runs, with SiO_2 and silicon targets, after normalization to the same neutron fluence.

The time-of-flight (TOF) obtained from the radio frequency of the cyclotron (stop signal for TDC) and the timing signal from each of the eight telescopes (start signal), is measured for each charged-particle event.

3. Data reduction procedures

The ΔE–E technique is used to identify light charged particles ranging from protons to lithium ions. Good separation of all particles is obtained over their entire energy range and therefore the particle identification procedure is straightforward.

Energy calibration of all detectors is obtained from the data itself [9,10]. Events in the ΔE–E bands are fitted with respect to the energy deposited in the two silicon detectors. This energy is determined from the detector thicknesses and calculations of energy loss in silicon. Supplementary calibration points are provided by transitions to the ground state and low-lying states in the H(n,p) reaction, as well as transitions to the ground state and low-lying states in the $^{12}C(n,d)^{11}B$, $^{16}O(n,d)^{15}N$ and $^{28}Si(n,d)^{27}Al$ reactions. The energy of each particle type is obtained by adding the energy deposited in each element of the telescope.

Low-energy charged particles are stopped in the ΔE_1 detector leading to a low-energy cutoff for particle identification of about 3 MeV for hydrogen isotopes and about 8 MeV for helium isotopes. The helium isotopes stopped in the ΔE_1 detector are nevertheless analyzed and a remarkably low cutoff, about 4 MeV, can be achieved for the experimental alpha-particle spectra. These alpha-particle events could obviously not be separated from ^{3}He events in the same energy region, but the yield of ^{3}He is much smaller than the alpha-particle yield in the region just above 8 MeV, where the particle identification works properly.

Knowing the energy calibration and the flight distances, the TOF for each charged particle from target to detector can be calculated and subtracted from the registered total TOF. The resulting neutron TOF is used for selection of charged-particle events induced by neutrons in the main peak of the incident neutron spectrum.

Absolute double-differential cross sections are obtained by normalizing the oxygen data to the number of recoil protons emerging from the CH_2 target. After selection of events in the main neutron peak and proper subtraction of the target-out and $^{12}C(n,px)$ background contributions, the latter taken from a previous experiment, the cross section can be determined from the recoil

proton peak, using *np* scattering data [8]. All data have been normalized using the *np* scattering peak in the 20° telescope.

Due to the finite target thickness, corrections for energy loss and particle loss are applied to both targets individually. Details of the correction methods are described in Refs. [9,10]. The cross sections for oxygen are obtained after subtraction of the silicon data from the SiO_2 data with proper normalization with respect to the number of silicon nuclei in the two targets.

4. Results and discussion

Double-differential cross sections at laboratory angles of 20°, 40°, 100° and 140° for protons and alpha particles, compared to the calculations based on the GNASH [11] and TALYS [12] models, are shown in Figs. 1-2, respectively. The error bars represent statistical uncertainties only. For protons above 25 MeV, both calculations give a reasonably good description of the spectra, although the calculated 20° cross sections, in particular the TALYS ones, fall below the experimental data. The low-energy statistical peak below 15 MeV in the spectra is considerably overpredicted by the two codes. The overestimate is particularly strong at backward angles for TALYS and at forward angles for GNASH.

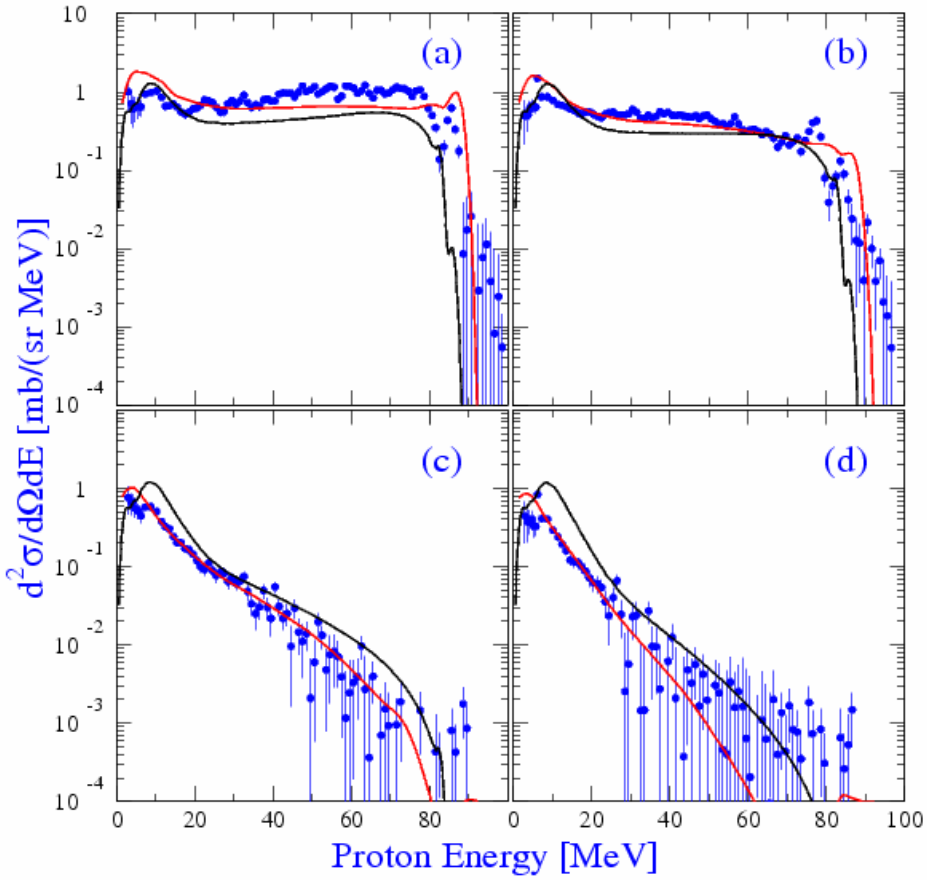

Fig. 1. Experimental double-differential cross sections (filled circles) of the O(n,px) reaction at 96 MeV at a) 20°, b) 40°, c) 100°, and d) 140°. The curves indicate theoretical calculations based on GNASH (red) and TALYS (black).

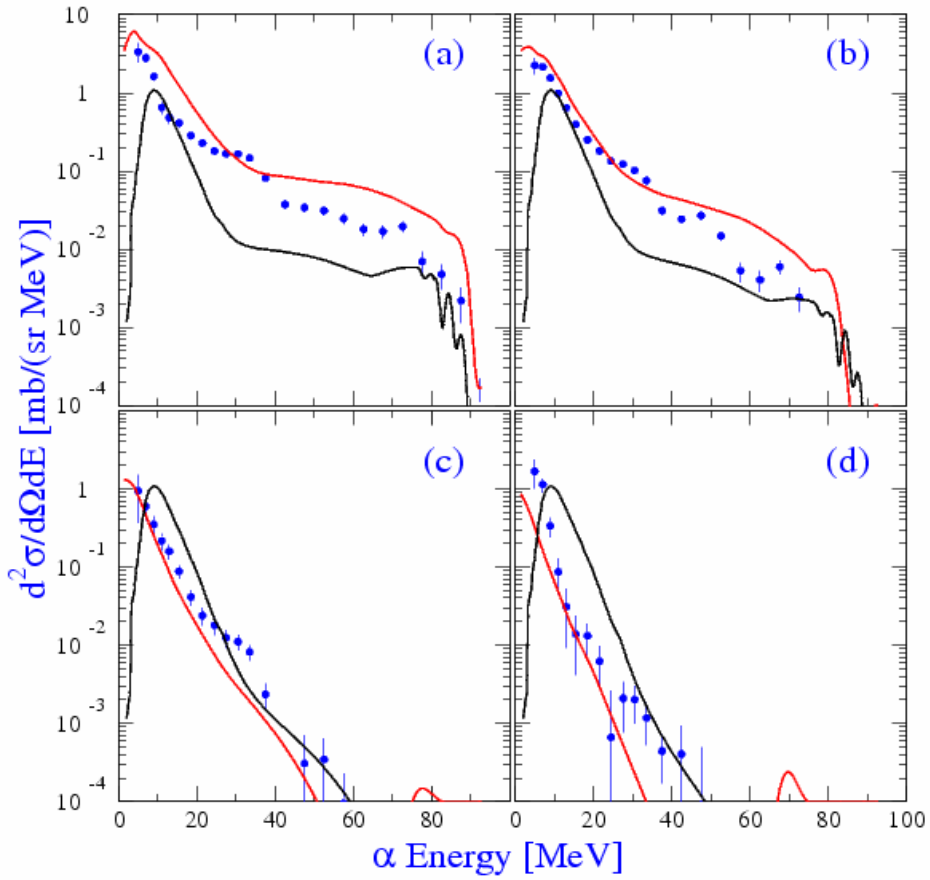

Fig. 2. Same as Fig. 1 for the O(n,αx) reactions.

The overall shapes of the alpha particle spectra (Fig. 2) are reasonably well described by the two models. The GNASH calculations, however, overpredict the cross sections at forward angles and underpredict them at large angles, whereas the TALYS calculations do the opposite, i.e., underpredict at small angles and overpredict at large angles.

By integration of the experimental angular distribution, energy-differential cross sections (dσ/dE) are obtained for each ejectile. These are shown in Fig. 3 together with theoretical calculations. For all ejectiles both calculations give a fair description of the energy dependence. Both calculations are in good agreement with the proton experimental data over the whole energy range, although the calculation for (n,px) reactions to discrete low-lying states underestimates the data. A study of the spectroscopic strengths for these states would be welcome. Concerning the deuteron spectra, the GNASH calculations are in good agreement with the data, whereas the TALYS code gives cross sections a factor of two or more larger than the experimental ones at energies above 30 MeV. In the case of alpha particles, the GNASH calculation tends to overpredict the high-energy part of the spectrum, and the TALYS calculations fall below the data above an alpha particle energy of 25 MeV. The energy dependence of the triton and ^{3}He spectra are well described by the TALYS code, but in both cases the calculation falls below the data above about 20 MeV.

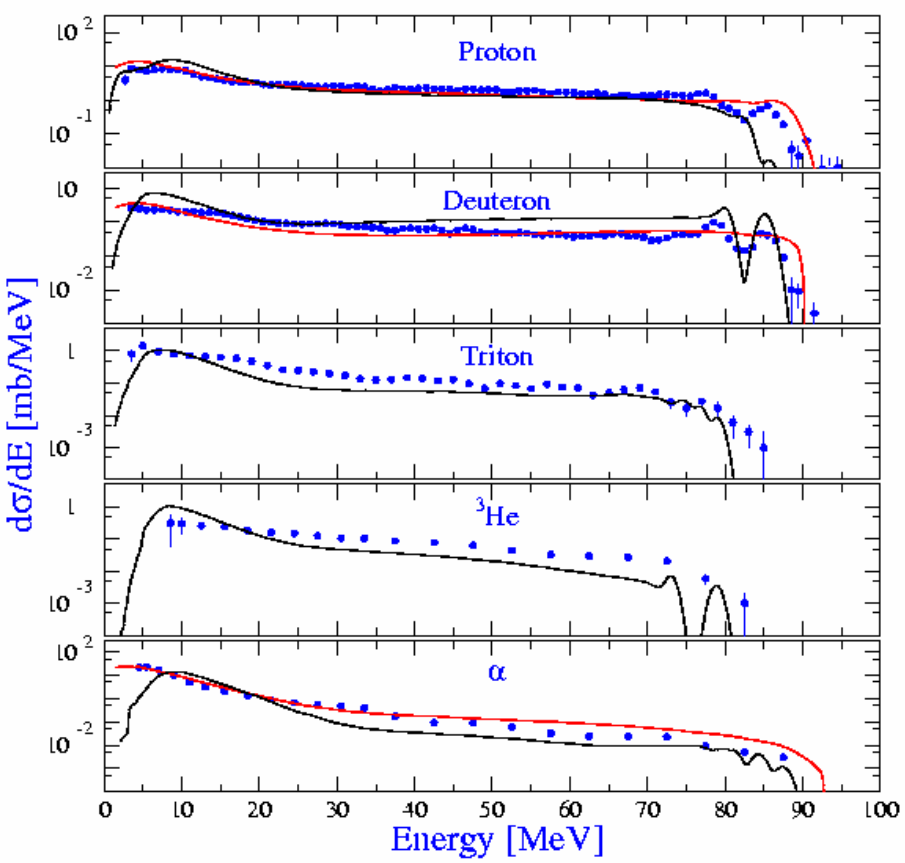

Fig. 3. Experimental energy-differential cross sections (filled circles) for neutron induced p, d, t, ^{3}He and alpha production at 96 MeV. The curves indicate theoretical calculations based on GNASH (red) and TALYS (black).

The production cross sections are deduced by integration of the energy differential spectra (see Table 1). To be compared with the calculated cross sections, the experimental values in Table 1 have to be corrected for the undetected particles below the low-energy cutoff. This is particularly important for ^{3}He because of the high cutoff energy. The corrections obtained with

TABLE 1. Experimental production cross sections for proton, deuteron, triton, ^{3}He and alpha particles from the present work. Theoretical values resulting from GNASH and TALYS calculations are given as well. The experimental data in the second column have been obtained with cutoff energies of 2.5, 3.0, 3.5, 8.0 and 4.0 MeV for p, d, t, ^{3}He and alpha particles, respectively. The third and forth columns show data corrected for these cutoffs, using the GNASH and TALYS calculation, respectively.

σ_{prod}	Experiment (mb)	Cutoff Corrected Experiment		Theoretical calculation	
		GNASH	TALYS	GNASH	TALYS
(n,px)	224 ± 11	248	231	259.9	221.7
(n,dx)	72 ± 4	80	73	73.4	131.3
(n,tx)	20± 1	—	20	—	10.6
(n, ^{3}Hex)	6.9 ± 0.6	—	8.7	—	8.2
(n,αx)	132 ± 7	218	132	224.7	88.4

TALYS seem to be too small in some cases, in particular for the (n,αx) production cross section. This is illustrated in Fig. 3, bottom panel, where the TALYS curve falls well below the experimental dσ/dE data in the 4–7 MeV region.

The proton, deuteron, triton, and alpha particle production cross sections are compared with previous data at lower energies [13] in Fig. 4. There seems to be general agreement between the trends of the previous data and the present data points. The curves in this figure are based on a GNASH calculation.

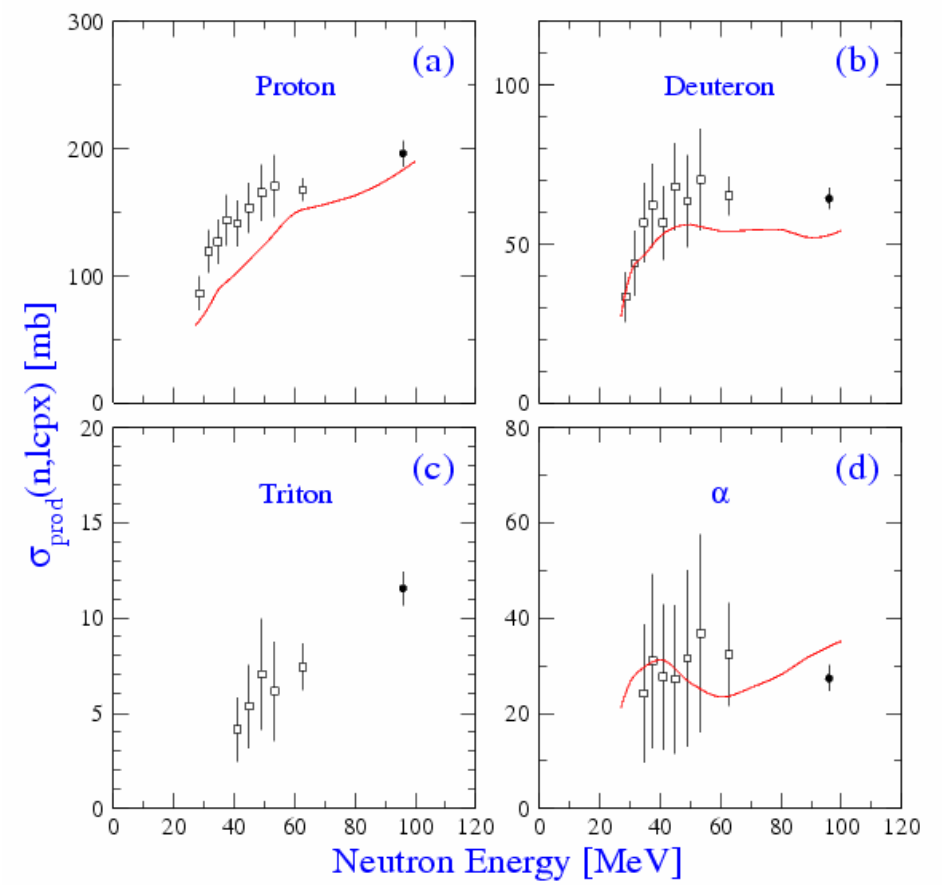

Fig. 4. Neutron-induced a) proton, b) deuteron, c) triton, and d) alpha particle production cross section as a function of neutron energy. The full circles are from the present work, whereas the open squares are from previous work [13]. The curves are based on a GNASH calculation. The data as well as the calculations correspond to cutoff energies of 6 MeV for protons and deuterons and 12 MeV for tritons and alpha particles. Note that the cutoff energies are different from those in Table 1.

5. Conclusion

In the present paper, an experimental data set on light-ion production in oxygen induced by 96 MeV neutrons is reported. Experimental double-differential cross sections are measured at eight angles between 20° and 160°. Energy-differential and production cross sections are obtained for the five types of outgoing particles. Theoretical calculations based on nuclear reaction codes including direct, pre-equilibrium and statistical models give generally a good

account of the magnitude of the experimental cross sections. For proton emission, the shape of the spectra for the double-differential and energy-differential cross sections are well described. The calculated and the experimental alpha-particle spectra are also in fair agreement with the exception of the high-energy part, where the GNASH model predicts higher yield and the TALYS model lower yield than experimentally observed. For the proton evaporation peak, the global TALYS calculation overestimates the data. For the other complex ejectiles, there are important differences between theory and experiment in what concerns the shape of the spectra at various angles.

Acknowledgements

This work was supported by the Swedish Natural Science Research Council, the Swedish Nuclear Fuel and Waste Management Company, the Swedish Nuclear Power Inspectorate, Ringhals AB, and the Swedish Defence Research Agency. The authors wish to thank the The Svedberg Laboratory for excellent support.

References

[1] D. O'Sullivan, D. Zhou and E. Flood, *Investigation of cosmic rays and their secondaries at aircraft altitudes*, Radiat. Meas. 34, 277–280 (2001).
[2] R. Orecchia, A. Zurlo, A. Loasses, M. Krengli, G. Tosi, S. Zurrida, P. Zucali, and U. Veronesi, *Particle Beam Therapy (Hadron therapy): Basis for Interest and Clinical Experience,* Eur. J. Cancer 34, 459 (1998).
[3] D.L. Schwartz, J. Einck, J. Bellon, and G.E. Laramore, *Fast Neutron Radiotherapy For Soft Tissue And Cartilaginous Sarcomas At High Risk For Local Recurrence*, Int. J. Radiat. Oncol. Biol. Phys. 50, 449 (2001).
[4] *Single-Event Upsets in Microelectronics*, topical issue, eds. H.H.K. Tang and N. Olsson, Mat. Res. Soc. Bull. 28 (2003).
[5] U. Tippawan, S. Pomp, A. Ataç, B. Bergenwall, J. Blomgren, S. Dangtip, A. Hildebrand, C. Johansson, J. Klug, P. Mermod, L. Nilsson, M. Österlund, N. Olsson, A.V. Prokofiev, P. Nadel-Turonski, V. Corcalciuc, and A. J. Koning, *Light-ion production in the interaction of 96 MeV neutrons with oxygen*, Phys. Rev. C 73, 034611 (2006).
[6] S. Dangtip, A. Ataç, B. Bergenwall, J. Blomgren, K. Elmgren, C. Johansson, J. Klug, N. Olsson, G. Alm Carlsson, J. Söderberg, O. Jonsson, L. Nilsson, P.-U. Renberg, P. Nadel-Turonski, C. Le Brun, F.R. Lecolley, J.F. Lecolley, C. Varignon, Ph. Eudes, F. Haddad, M. Kerveno, T. Kirchner, and C. Lebrun, *A facility for measurements of nuclear cross sections for fast neutron cancer therapy*, Nucl. Instr. Meth. Phys. Res. A 452, 484 (2000).
[7] J. Klug, J. Blomgren, A. Ataç, B. Bergenwall, S. Dangtip, K. Elmgren, C. Johansson, N. Olsson, S. Pomp, A.V. Prokofiev, J. Rahm, U. Tippawan, O. Jonsson, L. Nilsson, P.-U. Renberg, P. Nadel-Turonski, A. Ringbom, A. Oberstedt, F. Tovesson, V. Blideanu, C. Le Brun, J.F. Lecolley, F.R. Lecolley, M. Louvel, N. Marie, C. Schweitzer, C. Varignon, Ph. Eudes, F. Haddad, M. Kerveno, T. Kirchner, C. Lebrun, L. Stuttgé, I. Slypen, A. Smirnov, R. Michel, S. Neumann, and U. Herpers, *SCANDAL–a facility for elastic neutron scattering studies in the 50–130 MeV range*, Nucl. Instr. Meth. Phys. Res. A 489, 282 (2002).
[8] J. Rahm, J. Blomgren, H. Condé, S. Dangtip, K. Elmgren, N. Olsson, T. Rönnqvist, R. Zorro, O. Jonsson, L. Nilsson, P.-U. Renberg, A. Ringbom, G. Tibell, S.Y. van der Werf, T.E.O. Ericson, and B. Loiseau, *np scattering measurements at 96 MeV*, Phys. Rev. C 63, 044001 (2001).
[9] U. Tippawan, S. Pomp, A. Ataç, B. Bergenwall, J. Blomgren, S. Dangtip, A. Hildebrand, C. Johansson, J. Klug, P. Mermod, L. Nilsson, M. Österlund, N. Olsson, K. Elmgren, O. Jonsson,

A.V. Prokofiev, P.-U. Renberg, P. Nadel-Turonski, V. Corcalciuc, Y. Watanabe, and A. J. Koning, *Light-ion production in the interaction of 96 MeV neutrons with silicon*, Phys. Rev. C 69, 064609 (2004).

[10] U. Tippawan, *Secondary Particle Spectra from Neutron Induced Nuclear Reaction in the 14-100 MeV Region*, Doctoral thesis, Chiang Mai University (2004) (unpublished).

[11] ICRU Report 63, *International Commission on Radiation Units and Measurements*, Bethesda, MD, March 2000.

[12] A.J. Koning, S. Hilaire, and M.C. Duijvestijn, *TALYS-0.64 User Manual*, December 5, 2004, NRG Report 21297/04.62741/P FAI/AK/AK.

[13] S. Benck, I. Slypen, J.P. Meulders, and V. Corcalciuc, *Experimental double-differential cross sections and derived kerma factors for oxygen at incident neutron energies from reaction thresholds to 65 MeV*, Phys. Med. Biol. 43, 3427 (1998).